REFERENCES AND NOTES

1. W. A. Phillips, Ed., *Amorphous Solids: Low Temperature Properties* (Springer-Verlag, Berlin, 1981).
2. P. W. Anderson, B. I. Halperin, C. M. Varma, *Philos. Mag.* **25**, 1 (1972).
3. W. A. Phillips, *J. Low Temp. Phys.* 7, 351 (1972).
4. M. P. Zaitlin and A. C. Anderson, *Phys. Rev. B* **12**, 4475 (1975).
5. R. C. Zeller and R. O. Pohl, *ibid.* **4**, 2029 (1971).
6. E. Akkermans and R. Maynard, *ibid.* **32**, 7850 (1985).
7. S. Alexander, O. Entin-Wohlman, R. Orbach, *ibid.* **34**, 2726 (1986).
8. J. E. Graebner, B. Golding, L. C. Allen, *ibid.*, p. 5696.
9. C. C. Yu and J. J. Freeman, *ibid.* **36**, 7620 (1987).
10. G. A. Slack, in *Solid State Physics*, F. Seitz and D. Turnbull, Eds. (Academic Press, New York, 1979), vol. 34, p. 1.
11. A. Einstein, *Ann. Phys. (N.Y.)* **35**, 679 (1911).
12. D. G. Cahill and R. O. Pohl, *Annu. Rev. Phys. Chem.* **39**, 93 (1988).
13. D. G. Cahill, thesis, Cornell University (1989).
14. _____ and R. O. Pohl, *Solid State Commun.* **70**, 927 (1989).
15. P. B. Allen and J. L. Feldman, *Phys. Rev. Lett.* **62**, 645 (1989).
16. D. Stauffer, *Introduction to Percolation Theory* (Taylor & Francis, Philadelphia, 1985), p. 17.
17. G. F. Weir and G. J. Morgan, *J. Phys. F* **11**, 1833 (1981).
18. Increasing amount of fluctuation from one configuration to the next is seen for $p \leq 0.5$.
19. The phonon dispersion relation on a simple cubic lattice with $p = 1$ is given by

$$\omega^2 = 4\beta(3 - \sum_{i=1}^{3} \cos k_i a_0)/m$$

where k_i, $i = 1$ to 3, denotes the wave vector in either the x, y, or z direction.

20. Q. J. Chu and Z. Q. Zhang, *Phys. Rev. B* **39**, 7120 (1989).
21. R. Haydock, in *Solid State Physics*, H. Ehrenreich, F. Seitz, D. Turnbull, Eds. (Academic Press, New York, 1980), p. 216.
22. D. G. Cahill and R. O. Pohl, *Phys. Rev. B* **35**, 4067 (1987).
23. No literature value could be found. Therefore, we have used the value similar to PMMA.
24. C. A. Condat and T. R. Kirkpatrick, in *Scattering and Localization of Classical Waves in Random Media*, P. Sheng, Ed. (World Scientific, Singapore, 1990), p. 423.
25. We acknowledge helpful discussions with Z. Q. Zhang and useful comments on the manuscript by R. O. Pohl.

18 March 1991; accepted 3 June 1991

Quantification of Primary Versus Secondary C–H Bond Cleavage in Alkane Activation: Propane on Pt

W. HENRY WEINBERG* AND YONG-KUI SUN†

The trapping-mediated dissociative chemisorption of three isotopes of propane (C_3H_8, $CH_3CD_2CH_3$, and C_3D_8) has been investigated on the Pt(110)-(1 × 2) surface, and both the apparent activation energies and the preexponential factors of the surface reaction rate coefficients have been measured. In addition, the probabilities of primary and secondary C–H bond cleavage for alkane activation on a surface were evaluated. The activation energy for primary C–H bond cleavage was 425 calories per mole greater than that of secondary C–H bond cleavage, and the two true activation energies that embody the single measured activation energy were determined for each of the three isotopes. Secondary C–H bond cleavage is also preferred on entropic grounds, and the magnitude of the effect was quantified.

BOTH DUE TO ITS EXTREME TECHNOLOGICAL importance and its intrinsic scientific challenge, the activation of alkane molecules by both homogeneous transition metal complexes (*1*) and heterogeneous surfaces (*2–4*) has been a very active area of research during the past decade. Alkane activation by transition metal surfaces (C–H bond cleavage resulting in dissociative chemisorption) has been studied by both molecular beam scattering (*5–8*) as well as "bulb" chemical reaction (*9–13*) investigations. Two fundamentally different reaction mechanisms have emerged from these studies of alkane activation. These two mechanisms are the following: (i) direct dissociation; and (ii) trapping-mediated dissociative chemisorption.

Direct dissociative chemisorption occurs on the time scale of a collision between the gas-phase molecule and the surface ($\leq 10^{-12}$ s), and the rate of this reaction depends primarily on the translational and internal energies of the gas-phase molecule (and to a lesser extent on the temperature of the surface) (*3, 4*). In trapping-mediated dissociative chemisorption, the gas-phase molecule is trapped in the potential field of the surface (that is, it is adsorbed physically in the case of an alkane) and it accommodates to the temperature of the surface. The physically adsorbed molecule may then either desorb with a rate coefficient k_d (with an associated activation energy of desorption E_d) or it may react (dissociate) with a rate coefficient k_r [with an associated activation energy of reaction (E_r) (*4, 14–17*)]. The rate of this reaction is a function of the surface temperature. The gas temperature is important only insofar as it affects the probability of trapping into the physically adsorbed state. When a molecular beam of reactants with sufficiently high translational energy impinges on a surface, the direct mechanism would be favored primarily because the trapping probability becomes very small in this case. In a bulb rather than a beam environment, which one encounters more typically in technological processes, the trapping-mediated mechanism is expected to dominate. An exception to this rule would occur if $E_r - E_d$ were sufficiently large that the surface temperature would have to be so high for the reaction to occur that the residence time of the molecular adsorbate is too short for accommodation and reaction through this trapping-mediated mechanism. This appears to be the case, for example, for the dissociative adsorption of methane on low-index surfaces of nickel (*3, 6, 11*), but it is not the case for methane on the Pt(110)-(1 × 2) surface (*13*). For all alkanes with the possible exception of methane, in a bulb experiment with a Maxwell-Boltzmann distribution of velocities, one expects the trapping-mediated mechanism to dominate.

The results of an investigation of the dissociative chemisorption of propane on the reconstructed and highly corrugated Pt(110)-(1 × 2) surface (*10, 13, 18*) are reported here, where the trapping-mediated mechanism of chemisorption occurs. Three different isotopes of propane (C_3H_8, C_3D_8, and $CH_3CD_2CH_3$) were used to determine the relative probability of primary (1°) versus secondary (2°) C–H bond cleavage in linear alkanes such as propane, in which there are two inequivalent kinds of C–H bonds. Since the bond dissociation energy of the 1° C–H bonds in propane is 97.9 ± 1 kcal/mol whereas that of the 2° C–H bonds is 95.1 ± 1 kcal/mol (*19*), and because it seems unlikely that the bond dissociation energies of the two platinum-propyls that are formed in the reaction would have a difference that is this great, one might expect a priori a preference for the formation of $Pt–CH(CH_3)_2$ (*17*). Steric constraints might also favor one reaction product over the other in a heretofore unknown way. This is an important issue which has rather profound mechanistic implications insofar as selectivity in heterogeneous catalysis is concerned. As discussed below, a propensity for the 2° C–H bond-cleavage reaction for propane on this surface of platinum has been confirmed and quantified.

The measurements were carried out in an ion-pumped ultrahigh vacuum (UHV) microreactor (base pressure of 3×10^{-10} torr, volume of 30 cm^3) (*13, 20*). The experi-

---

Department of Chemical Engineering, University of California, Santa Barbara, Santa Barbara, CA 93106.

*To whom correspondence should be addressed.
†Present address: Department of Chemistry BG-10, University of Washington, Seattle, WA 98195.

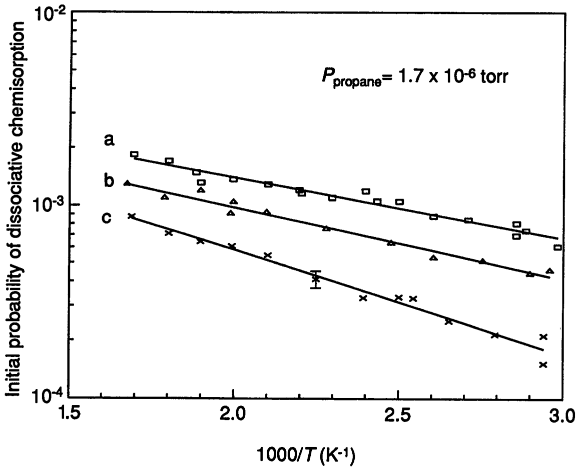

Fig. 1. Initial probabilities of trapping-mediated dissociative chemisorption of (a) C_3H_8, (b) $CH_3CD_2CH_3$, and (c) C_3D_8 on Pt(110)-(1 × 2) as a function of reciprocal surface temperature. The slopes ($-E/k_B$) and the intercepts $k_r^{(0)}/k_d^{(0)}$ of these three lines are listed in Table 1. The error bar represents the maximum variation in the measured rate at each temperature.

ments were carried out by flowing propane at a pressure of 1.7×10^{-6} torr (a calibrated flux) through the microreactor for a reaction time τ at various constant surface temperatures with a flow rate that is much greater than the rate of dissociation of the propane (in order to maintain low conversions of the propane). The surface temperature was varied between 335 and 610 K, whereas the gas temperature was always equal to the wall temperature of the reactor, ~300 K, since the mean-free path of the propane is much longer than the dimensions of the microreactor. The number of carbon atoms on the surface after the reaction N_c, which is proportional to the probability of dissociative chemisorption (*21*), was determined after evacuation of the propane by counting mass spectrometrically the number of CO_2 molecules that are produced by titrating the surface carbon atoms with oxygen. The surface carbon was fully oxidized to CO_2 under the titration conditions, and a number of measurements were carried out with ^{13}C-labeled hydrocarbons to show that the oxidation of background CO to CO_2 during the titration contributes negligibly to the measured CO_2. The pressure of propane and the reaction time (τ) were chosen such that the final coverage of carbon was between ~5 and 8% of a monolayer of carbidic carbon. The lower limit ensures that our results were not dominated by reactivity at surface defects, whereas the upper limit ensures that we measured approximately the initial rate of the activation reaction, that is, the rate characteristic of a clean Pt(110)-(1 × 2) surface. The probability of dissociative chemisorption is given by

$$P_r = N_c/3\tau F \tag{1}$$

where F is the impingement flux of propane onto the surface on a per-site basis, and the factor of 3 in the denominator accounts for the fact that there are three carbon atoms per propane molecule.

The measured values of $\ln(P_r)$ as a function of reciprocal surface temperature are shown in Fig. 1 for C_3H_8 (line a), $CH_3CD_2CH_3$ (line b), and C_3D_8 (line c). Three important conclusions may be drawn from the data of Fig. 1. First, since the reaction probability varies with surface temperature while the gas temperature is constant, the reaction clearly obeys a trapping-mediated mechanism, as anticipated above. Second, both 1° and 2° C–H bond cleavages occur in the dissociation of propane on the Pt(110)-(1 × 2) surface. This is seen easily from the following considerations. If only 1° C–H bond cleavage were occurring, then line b would fall on top of line a in Fig 1; whereas if only 2° C–H bond cleavage were occurring, then line b would fall on top of line c. Line b falls between lines a and c, however, which implies that some of the propane molecules react through 1° C–H bond cleavage, and the others that react do so through 2° C–H bond cleavage (*22*). A quantification of these two probabilities is presented below. Third, because of the linearity of these Arrhenius constructions, the reaction probability P_r may be written as

$$P_r = P_r^{(0)} e^{-E/k_B T} \tag{2}$$

where k_B is Boltzmann's constant and T is the absolute temperature, with apparent activation energies E given by 1460 ± 200, 1800 ± 200, and 2330 ± 200 cal/mol for C_3H_8, $CH_3CD_2CH_3$, and C_3D_8, respectively. The uncertainties represent one standard deviation of a linear least squares fit to all of the measured data. The apparent preexponential factor $P_r^{(0)}$ is 6.1×10^{-3} for all three isotopes.

In order to attach microscopic significance to these rate parameters, it is necessary to consider the mechanism of trapping-mediated chemisorption, namely,

$$CH_3CH_2CH_3(g) \underset{k_d}{\overset{\xi F}{\rightleftarrows}} CH_3CH_2CH_3(a)$$

$$CH_3CH_2CH_3(a) \xrightarrow{k_{r1}} CH_3CH_2CH_2(a) + H(a)$$

$$CH_3CH_2CH_3(a) \xrightarrow{k_{r2}} CH_3CHCH_3(a) + H(a)$$

where ξ is the thermally averaged trapping probability of the propane, which is approximately equal to unity under our experimental conditions (*4*), k_d is the first-order desorption rate coefficient of the physically adsorbed propane, and k_{r1} and k_{r2} are the reaction rate coefficients for 1° and 2° C–H bond cleavage, respectively. Since the fractional surface coverage of molecularly adsorbed propane was extremely small (the maximum fractional coverage, which occurs at 335 K, is estimated to be $\sim 10^{-7}$), a pseudo-steady-state analysis could be used to determine the fractional coverage of the adsorbed propane, and from this the probability of reaction (the ratio of the rate of reaction to the rate of impingement) is given by (*4, 8, 15*)

$$P_r = \frac{k_{r1} + k_{r2}}{k_{r1} + k_{r2} + k_d} \tag{3}$$

Since $P_r << 1$ (compare with Fig. 1), it follows that Eq. 3 may be written as

$$P_r = \frac{k_{r1} + k_{r2}}{k_d} \tag{4}$$

On the basis of Eq. 4, one might expect nonlinear Arrhenius plots in Fig. 1, which, however, is not the case. Consequently, at

Table 1. Rate parameters for the dissociative chemisorption of propane on Pt(110)-(1 × 2). The separately measured value of the desorption rate coefficient (*10*), $k_d = 10^{13}\, e^{-(9700 \text{ cal/mol})/k_B T}\ s^{-1}$, was used in evaluating E_r and $k_r^{(0)}$. As discussed in the text, $E_r - E_d$ is the apparent activation energy (with respect to a gas-phase energy zero) of dissociative chemisorption of the three isotopes of propane, whereas $E_r^{(1°)} - E_d$ and $E_r^{(2°)} - E_d$ are the true activation energies of 1° and 2° C–H bond dissociation, respectively (with respect to the same gas-phase energy zero).

Reactant	$E = E_r - E_d$ (cal/mol)	$k_r^{(0)}/k_d^{(0)}$	E_r (cal/mol)	$k_r^{(0)}$ (s^{-1})	$E_r^{(1°)} - E_d$ (cal/mol)	$E_r^{(2°)} - E_d$ (cal/mol)
C_3H_8	1,460	6.1×10^{-3}	11,160	6.1×10^{10}	1,650	1,225
$CH_3CD_2CH_3$	1,800	6.1×10^{-3}	11,500	6.1×10^{10}	1,650	2,095
C_3D_8	2,330	6.1×10^{-3}	12,030	6.1×10^{10}	2,520	2,095

the level of "resolution" of Fig. 1, Eq. 4 may be rewritten as

$$P_r = \frac{k_r}{k_d} \qquad (5)$$

where k_r is an averaged (apparent) rate coefficient for the dissociation reaction, considering the cleavage of both 1° and 2° C–H bonds. Note that Eq. 5 serves to quantify the rate parameters reported above, namely, $E \equiv E_r - E_d$ and $P_r^{(0)} \equiv k_r^{(0)}/k_d^{(0)}$, where $k_r^{(0)}$ and $k_d^{(0)}$ are the preexponential factors of the two reaction-rate coefficients. Since the rate coefficient of desorption of molecular propane from Pt(110)-(1 × 2) has been found to be $k_d = 10^{13}e^{-(9700\ \mathrm{cal/mol})/k_BT}\ \mathrm{s}^{-1}$ (*10*), a quantification of the preexponential factor ($k_r^{(0)}$) and the activation energy (E_r) of the surface dissociation reaction is possible. (Note that E_r is measured with respect to the ground state of the physically adsorbed well.) These rate parameters for the three isotopes of propane are collected in Table 1, and, as expected (*4, 17*), the ratio $k_r^{(0)}/k_d^{(0)}$ is both independent of the isotope and much less than unity.

We used the data of Fig. 1 to determine the probability of 1° and 2° C–H bond cleavage in reacting propane. We define $P_{r,i}$, to be the probability of reaction of the ith isotope of propane, $\tilde{P}_p$ to be the conditional probability of formation of a 1° Pt-propyl given that the propane reacts, and $\tilde{P}_s = 1 - \tilde{P}_p$ to be the conditional probability of formation of a 2° Pt-propyl given that the propane reacts. Thus, it follows that

$$P_{r,C_3H_8}\tilde{P}_p + \tilde{P}_{r,C_3D_8}\tilde{P}_s = P_{r,CH_3CD_2CH_3} \qquad (6)$$

where the $P_{r,i}$ are given, as a function of temperature, in Fig. 1. Solving Eq. 6 gives both $\tilde{P}_p(T)$ and $\tilde{P}_s(T) = 1 - \tilde{P}_p(T)$; these probabilities refer to a pure isotope of propane (C_3H_8 or C_3D_8). It is instructive to introduce a related conditional probability P_p which is that of cleavage of a 1° C–H bond, given that the propane molecule reacts ($P_s = 1 - P_p$ is defined analogously). The two probabilities, $\tilde{P}_p$ and $\tilde{P}_p$, are related by the number of 1° and 2° hydrogen atoms in propane:

$$\frac{6P_p}{6P_p + 2P_s} = \tilde{P}_p \qquad (7)$$

which permits an evaluation of $P_p(T)$ and $P_s(T)$. All of these probabilities (P_p, $\tilde{P}_p$, P_s, and $\tilde{P}_s$) may be written exactly in the form $P = P^{(0)}e^{-\Delta E/k_BT}$. The derived slopes and intercepts of the four Arrhenius constructions implied by this relation are the following:

$$P_p = 0.34\,e^{-(325\ \mathrm{cal/mol})/k_BT} \qquad (8)$$

$$P_s = 0.66\,e^{+(100\ \mathrm{cal/mol})/k_BT} \qquad (9)$$

$$\tilde{P}_p = 0.61\,e^{-(220\ \mathrm{cal/mol})/k_BT} \qquad (10)$$

$$\tilde{P}_s = 0.39\,e^{+(205\ \mathrm{cal/mol})/k_BT} \qquad (11)$$

Equations 8 to 11 quantify the probabilities of 1° versus 2° C–H bond cleavage and 1° versus 2° Pt-propyl formation for a pure isotope of propane. By taking ratios of these probabilities, the difference in the activation energies for 1° and 2° C–H bond cleavage may be determined:

$$\frac{P_p}{P_s} = 0.52\,e^{-(425\ \mathrm{cal/mol})/k_BT} \qquad (12)$$

$$\frac{\tilde{P}_p}{\tilde{P}_s} = 1.56\,e^{-(425\ \mathrm{cal/mol})/k_BT} \qquad (13)$$

Equations 12 and 13 imply that the difference in activation energy of 1° and 2° C–H bond cleavage, $E_r^{(1°)} - E_r^{(2°)}$, is 425 cal/mol, and the data of Fig. 1 imply directly that the difference in activation energy of C–D and C–H bond cleavage, $E_r^{(D)} - E_r^{(H)}$, is 870 cal/mol. With these constraints it is possible to determine values of the two activation energies that are contained within the single apparent value derived from Fig. 1 for each isotope and reported, for example, as $E_r - E_d$ in the second column of Table 1. Varying $E_r^{(1°)}$ and $E_r^{(2°)}$ with the two constraints delineated above was carried out with the goal of reproducing, self-consistently, the measured data shown in Fig. 1 for all three isotopes of propane. The values of $E_r^{(1°)}$ and $E_r^{(2°)}$, expressed as $E_r^{(1°)} - E_d$ and $E_r^{(2°)} - E_d$, that are reported in the sixth and seventh columns of Table 1, reproduced the experimental data of Fig. 1 to within 1.5% for all three isotopes over the entire temperature range. This is well within the experimental uncertainty of the data. Noticeable disagreement with the experimental data occurs if these energies are varied from their optimized values by as little as 50 cal/mol.

Finally, it is also important to note that the preexponential factors of Eqs. 12 and 13 give the ratio of conditional probabilities that apply in the limit of infinite temperature. This allows an assessment to be made of "steric" or entropic effects in the reaction. If the entropic factors were identical for the two reactions, then $\lim_{T\to\infty} P_p/P_s = 1$ and $\lim_{T\to\infty} \tilde{P}_p/\tilde{P}_s = 3$. Consequently, entropy also favors 2° C–H bond cleavage on this surface to the extent that the preexponential factor of Eq. 9 is 0.66 rather than 0.5, and the preexponential factor of Eq. 11 is 0.39 rather than 0.25.

The methodology that has been developed and presented here should have broad applications to the analysis of surface chemical reactivity that extend far beyond the specific, but important example of alkane activation. If linear Arrhenius constructions, such as those of Fig. 1, are observed experimentally, then all that is required is for a selectively deuterated reactant to give a statistically different rate compared to the perhydrido- and perdeutero-reactants. This scenario would be expected to be observed frequently (*23*).

REFERENCES AND NOTES

1. A. E. Shilov, *Activation of Saturated Hydrocarbons by Transition Metal Complexes* (Reidel, Boston, 1984); R. H. Crabtree, *Chem. Rev.* **85**, 245 (1985); B. Meunier and B. Chaudret, Eds., *Perspectives in the Selective Activation of C–H and C–C Bonds in Saturated Hydrocarbons*, vol. CXXX of the *NATO ASI Series* (Reidel, Dordrecht, 1987).
2. W. H. Weinberg, in *Survey of Progress in Chemistry*, A. Scott and G. Wubbel, Eds. (Academic Press, New York, 1983), vol. 10, pp. 1–59; R. Pitchai and K. Klier, *Catal. Rev. Sci. Eng.* **28**, 13 (1986).
3. S. T. Ceyer, *Annu. Rev. Phys. Chem.* **39**, 479 (1988).
4. W. H. Weinberg, in *Dynamics of Gas-Surface Collisions*, C. T. Rettner and M. N. R. Ashfold, Eds. (Royal Society of Chemistry, Cambridge, 1991), pp. 171–220.
5. C. T. Rettner, H. E. Pfnür, D. J. Auerbach, *Phys. Rev. Lett.* **54**, 2716 (1985); A. V. Hamza, H.-P., Steinrück, R. J. Madix, *J. Chem. Phys.* **86, 6506** (1987).
6. M. B. Lee, Q. Y. Yang, S. T. Ceyer, *J. Chem. Phys.* **87**, 2724 (1987).
7. A. C. Luntz and D. S. Bethune, *ibid.* **90**, 1274 (1989).
8. C. B. Mullins and W. H. Weinberg, *ibid.* **92**, 4508 (1990).
9. T. S. Wittrig, P. D. Szuromi, W. H. Weinberg, *ibid.* **76**, 3305 (1982); P. D. Szuromi, J. R. Engstrom, W. H. Weinberg, *ibid.* **80,** 508 (1984); P. D. Szuromi and W. H. Weinberg, *Surf. Sci.* **149**, 226 (1985).
10. P. D. Szuromi, J. R. Engstrom, W. H. Weinberg, *J. Phys. Chem.* **89**, 2497 (1985).
11. T. P. Beebe, Jr., D. W. Goodman, B. D. Kay, J. T. Yates, Jr., *J. Chem. Phys.* **87**, 2305 (1987).
12. S. G. Brass and G. Ehrlich, *ibid.*, p. 4285; A. G. Sault and D. W. Goodman, *ibid.* **88**, 7232 (1988); X. Jiang and D. W. Goodman, *Appl. Phys.* **A51**, 99 (1990); J. A. Rodriquez and D. W. Goodman, *J. Phys. Chem.* **94**, 5342 (1990).
13. Y.-K. Sun and W. H. Weinberg, *J. Vac. Sci. Technol.* **A8**, 2445 (1990).
14. E. S. Hood, B. H. Toby, W. H. Weinberg, *Phys. Rev. Lett.* **55**, 2437 (1985).
15. S. G. Brass and G. Ehrlich, *ibid.* **57**, 2532 (1986); W. H. Weinberg, in *Kinetics of Interface Reactions*, H. J. Kreuzer and M. Grunze, Eds. (Springer-Verlag, Heidelberg, 1987), pp. 94–121.
16. G. Ehrlich, in *Chemistry and Physics of Solid Surfaces VII*, R. Vanselow and R. F. Howe, Eds. (Springer-Verlag, Heidelberg, 1989), pp. 1–64.
17. C. T. Campbell, Y.-K. Sun, W. H. Weinberg, *Chem. Phys. Lett.* **179**, 53 (1991).
18. M. A. Van Hove, W. H. Weinberg, C. M. Chan, *Low-Energy Electron Diffraction: Experiment, Theory and Surface Structural Determination* (Springer-Verlag, Berlin, 1986).
19. D. F. McMillen and D. M. Golden, *Annu. Rev. Phys. Chem.* **33**, 493 (1982).
20. J. J. Vajo, W. Tsai, W. H. Weinberg, *Rev. Sci. Instrum.* **56**, 1439 (1985). The Pt(110) crystal was polished on both sides and was initially cleaned by Ar^+ sputtering and oxidation-reduction cycles in situ in the microreactor. The (1 × 2) reconstruction of the surface, following this cleaning procedure, was verified by low-energy electron diffraction in a separate UHV chamber. The surface of the crystal was cleaned between experiments by heating to 950 K for 5 min in 5×10^{-4} torr of O_2 flowing through

the microreactor, and subsequently in 5×10^{-4} torr of flowing H_2 for another 5 min to remove all surface oxygen. Thermal desorption spectra of CO from the surface, which were in complete agreement with previously published ones from the clean Pt(110)-(1 × 2) surface [C. M. Comrie and R. M. Lambert, *J. Chem. Soc. Faraday Trans.* **72**, 325 (1975)], were measured frequently in order to verify the cleanliness of the surface. Furthermore, all of the data concerning propane activation presented here were reproducible, indicating the absence of surface contamination. The C_3H_8 (99.5%) was obtained from Matheson, and both the $CH_3CD_2CH_3$ (98% by atom D) and the C_3D_8 (99.5% by atom D) were obtained from MSD Isotopes. All gases were stored and manipulated in a manifold that was pumped by a diffusion pump and which had a base pressure below 10^{-7} torr.

21. Under these experimental conditions the dissociative chemisorption of propane is irreversible, and no gas-phase carbon-containing products of a surface self-hydrogenolysis reaction are produced.
22. Note also that the observed kinetic isotope effect implies that C–H rather than C–C bond cleavage is occurring in the initial dissociative chemisorption, as would be expected. Furthermore, we have shown previously that the initial C–H bond-cleavage reaction is rate limiting in alkane activation (*9, 10, 17*).
23. If curved Arrhenius constructions are observed, then the raw data may be used directly to extract $\bar{E}_{r1}$ and E_{r2} via Eq. 4.
24. The support of this work by the Department of Energy (grant DE-FG03-89ER14048) and the Donors of The Petroleum Research Fund administered by the American Chemical Society (grant ACS-PRF-23801-AC5-C) is gratefully acknowledged.

15 April 1991; accepted 17 June 1991

Dimerization of Human Growth Hormone by Zinc

BRIAN C. CUNNINGHAM, MICHAEL G. MULKERRIN, JAMES A. WELLS*

Size-exclusion chromatography and sedimentation equilibrium studies demonstrated that zinc ion (Zn^{2+}) induced the dimerization of human growth hormone (hGH). Scatchard analysis of $^{65}Zn^{2+}$ binding to hGH showed that two Zn^{2+} ions associate per dimer of hGH in a cooperative fashion. Cobalt (II) can substitute for Zn^{2+} in the hormone dimer and gives a visible spectrum characteristic of cobalt coordinated in a tetrahedral fashion by oxygen- and nitrogen-containing ligands. Replacement of potential Zn^{2+} ligands (His^{18}, His^{21}, and Glu^{174}) in hGH with alanine weakened both Zn^{2+} binding and hGH dimer formation. The Zn^{2+}-hGH dimer was more stable than monomeric hGH to denaturation in guanidine-HCl. Formation of a Zn^{2+}-hGH dimeric complex may be important for storage of hGH in secretory granules.

HUMAN GROWTH HORMONE (hGH) is synthesized and secreted into storage granules before its release from the anterior pituitary (*1, 2*). Histochemical analysis of the anterior pituitary indicates that Zn^{2+} is present in high concentrations in growth hormone secretory granules (*3*). It has been suggested that Zn^{2+} may modulate release of growth hormone because high concentrations of Zn^{2+} inhibit growth hormone release (*4–6*). However, the biochemical and structural basis whereby Zn^{2+} functions in storage or release of hGH has not been elucidated.

After analyzing the binding of Zn^{2+} in the complex between hGH and the extracellular domain of the human prolactin receptor (hPRLbp) [K_d (dissociation constant) = 0.03 nM] (*7*), we measured the binding affinity of Zn^{2+} to each protein separately. Equilibrium dialysis showed no specific binding of $^{65}Zn^{2+}$ to the hPRLbp, whereas Scatchard analyses of binding studies performed at two different concentrations of hGH (3.3 μM and 4.8 μM) showed that Zn^{2+} forms a 1:1 complex with hGH (Fig. 1). The Scatchard plots curved upward, indicating that binding of one Zn^{2+} ion promotes the binding of another Zn^{2+} ion (positive cooperativity). From the linear portions of these plots, we estimate an apparent K_d for the higher affinity Zn^{2+} site of about 1 μM. Cooperative binding with a stoichiometry of 1:1 could be explained if Zn^{2+} induced hGH to oligomerize.

We used size exclusion chromatography to determine if Zn^{2+} did indeed induce oligomerization of hGH. Gel filtration of hGH (15 μM) in EDTA (Fig. 2) showed that hGH elutes as a symmetrical peak at a position corresponding to a molecular size of ~20 kD, approximately the size of monomeric hGH (22 kD). However, in the presence of $ZnCl_2$ (50 μM) the hormone chromatographed with an apparent molecular size that is 50% larger than in EDTA. The asymmetry of this peak is characteristic of a species that is dissociating on the column (*8*). At higher concentrations of hGH and $ZnCl_2$ (~150 μM), the hGH chromatographed as a more symmetrical peak with an apparent molecular size that is 1.85 times the monomeric hGH peak (*9*). Thus, at higher concentrations the dimerization is essentially complete. At lower concentrations (0.15 μM), hGH runs only as a monomer (*9*). These data indicate that at concentrations of hGH greater than micromolar, Zn^{2+} is able to promote the formation of an hGH dimer.

Sedimentation equilibrium studies (Fig. 3) confirm that hGH forms a dimeric complex (~44 kD) in the presence of, but not in the absence of, $ZnCl_2$. Moreover, the concentration dependence for dimer formation allowed us to calculate an apparent dimerization equilibrium constant for hGH (± SD) of 2.6 ± 0.1 μM in 20 μM $ZnCl_2$ (Table 1).

To probe the structural environment of the Zn^{2+} sites in the hGH dimer, we substituted Co^{2+}, a spectroscopically active metal (*10, 11*), for Zn^{2+}. Gel filtration experiments showed that Co^{2+} also induces dimerization of hGH (*9*). Moreover, both Zn^{2+} and Co^{2+} produce similar ultraviolet difference spectra on dimerization of the hormone (*9*), suggesting that the Zn^{2+} and Co^{2+} hGH complexes are structurally similar, if not identical.

Titration of hGH with Co^{2+} produces a visible absorption spectrum with a maxi-

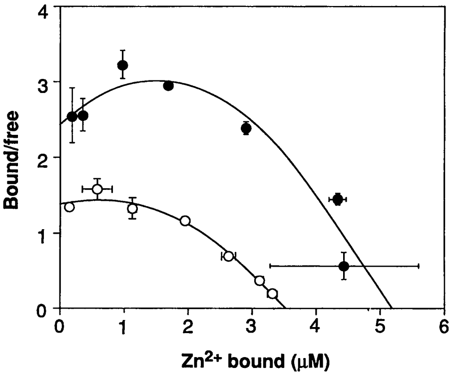

Fig. 1. Equilibrium dialysis and Scatchard analysis for binding of $^{65}Zn^{2+}$ to hGH (○, 3.3 μM; ●, 4.8 μM). We took precautions to minimize Zn^{2+} contamination in the buffers and dialysis cells as described (*7*). The hGH was mixed with dialysis buffer that contained tris, pH 7.5 (20 mM); NaCl (140 mM); and $MgCl_2$ (10 mM). We added the $MgCl_2$ to reduce nonspecific binding of Zn^{2+} to the dialysis cell membrane and hGH. The $MgCl_2$ neither promoted nor inhibited dimerization of hGH (*9*). Aliquots (100 μl) of the solution that contained hGH (3.3 or 4.8 μM) were added to one side of the dialysis cell. Serial dilutions (in triplicate) of unlabeled $ZnCl_2$ that contained 0.3 μM $^{65}ZnCl_2$ (eight dilution steps ranging from 0 to a final $ZnCl_2$ concentration of 40 μM) were added to the other side of the dialysis cell. Cells were rotated slowly for 16 to 20 hours at 25°C. Control experiments indicated this was sufficient time to reach equilibrium. Aliquots (50 μl) from each side of the dialysis cell were diluted into scintillation cocktail and analyzed for $^{65}Zn^{2+}$ content. From these values the concentrations of bound and free Zn^{2+} were calculated. Error bars indicate SD from triplicate determinations.

Department of Protein Engineering, Genentech, South San Francisco, CA 94080.

*To whom correspondence should be addressed.